Synthesis of carbon nanofibers by catalytic pyrolysis of ethylene in the presence of vapors of volatile components

A. A. Volodin, E. V. Gerasimova, and B. P. Tarasov*

Institute of Problems of Chemical Physics, Russian Academy of Sciences, 1 prosp. Akad. Semenova, 142432 Chernogolovka, Moscow Region, Russian Federation. Fax: +7 (496) 522 5401. E-mail: alexvol@icp.ac.ru

Catalytic pyrolysis of ethylene was carried out at 700 °C in the presence of vapors of H_2O, EtOH, NH_4OH, PCl_3, $(MeO)_3P$, Me_2SO_4, $(MeO)_3B$, and HCl. The composition of solid pyrolysis products was studied using the elemental analysis, X-ray diffraction analysis, and electron microscopy. The composition of the gaseous pyrolysis products was studied using mass spectrometry. The processes in the gas phase were characterized, and the relationship between conditions of ethylene pyrolysis and the structure of formed carbon nanofibers was revealed. The introduction of gaseous additives has a substantial effect on the formation, growth, and structure of the carbon nanofibers formed.

Key words: synthesis, pyrolysis, ethylene, gaseous additives, carbon nanofibers.

The introduction of various additives during synthesis of carbon nanostructures by catalytic decomposition of hydrocarbons can change both the yield of the target product and its structure.[1—7] Hydrogen and argon are often additionally introduced into the reaction medium. It is believed that hydrogen introduced into the pyrolysis zone interacts with adsorbed carbon on the surface of the catalytic particle to transfer the carbon to the gas phase, inhibiting coke formation on the working surface of the catalyst and increases the yield of the target product.[1] Argon is usually used as a diluting gas for decreasing the partial pressure of hydrocarbon.[2] The introduction of small amounts of oxygen removes amorphous carbon.[3] It was assumed[4] that an ammonia additive to the gas mixture passivates the catalytic particle surface and prevents fast coke formation on the catalyst. A similar effect is observed upon the addition of water vapor.[5,6] In addition, the presence of water in the reaction medium favors the growth of open nanotubes. The introduction of a CO admixture to gaseous hydrocarbon enhances the yield of carbon fiber.[7]

The introduction of various additives to the gas phase can change the structure of filamentous carbon formed upon catalytic pyrolysis. For example, the pyrolysis of acetylene at 900 °C in the presence of ferrocene as a procatalyst affords mainly single-wall nanotubes.[8] The introduction of sulfur into the reaction medium results in the predominant formation of double-wall nanotubes.[9] Double- and triple-wall nanotubes can be obtained using urea or citric acid as the starting compound.[10] The pyrolysis of methane on the Fe catalyst synthesized from $Fe_3(CO)_{12}$ in the presence of phosphorus compounds, which are introduced from a solution of H_3PO_4 in ethanol, in high yield produces carbon fibers up to 6 cm long.[11] The addition of chlorine-containing precursors, for instance, CH_2Cl_2, to acetylene gave bamboo-like nanotubes.[12] Nitrogen-containing carbon nanotubes of the same type were synthesized by the pyrolysis of dimethyl formamide.[13] The preliminary treatment of a mixture of B and BN powders in a ball mill for several hours followed by heating of the mixture for 1000—1200 °C in an NH_3 atmosphere in the presence of the procatalyst $FeCl_2 \cdot 4H_2O$ afforded bamboo-like boron nitride nanotubes.[14] Spiral nanotubes were synthesized by the pyrolysis of diethyl ether on the zinc catalyst.[15]

The introduction of various additives can change not only the structure and yield of carbon nanostructures but also their properties. The nanotubes with a large content of SO_3H groups were obtained, which possess both electron and proton conductivity.[16] Thus, the literature data and the results of our previous works[17,18] show that even insignificant amounts of various additives introduced into the reaction zone can exert a substantial effect on the yield, structure, and properties of the carbon nanostructures formed.

In the present work, we studied the influence of various gaseous additives to ethylene during its pyrolysis on the yield and structure of the produced carbon nanotubes.

Experimental

For catalyst preparation $Ni(NO_3)_2 \cdot 6H_2O$ (analytical pure grade, GOST 4055-78) and MgO (analytical pure grade, GOST 4526-75) were used. A solution of the weighed sample of $Ni(NO_3)_2 \cdot 6H_2O$ in distilled water was poured to MgO powder.

Published in Russian in *Izvestiya Akademii Nauk. Seriya Khimicheskaya,* No. 3, pp. 398—403, March, 2011.

The resulting suspension was treated in an ultrasonic bath for 30 min. Then the suspension was evaporated and dried for 1 h in air at 150 °C. The metal was reduced directly during pyrolysis without preliminary storage in a hydrogen atmosphere. We have found earlier[19] that the optimal growth of carbon fibers was observed at a Ni catalyst content of 5 wt.%. At a lower metal concentration, the yield of carbon pyrolysis products decreases considerably, while at a higher concentration a large amount of amorphous carbon and encapsulated particles is formed. The nickel content on the support (5 wt.%) was confirmed by elemental analysis data.

Catalytic pyrolysis of ethylene was carried out in a horizontal quartz flow-type reactor at atmospheric pressure at 700 °C for 1 h. A quartz boat with the catalyst was placed in the center of the reactor. A C_2H_4—H_2—Ar (1.5 : 3 : 1, vol.) gas mixture was used during pyrolysis. Gaseous additives were introduced into the reaction zone by bubbling an argon flow through a bubbler flask filled with the liquid component. The amount of the gaseous additive correlating with the saturation vapor pressure was controlled by a change in the temperature of the bubbler flask. The following additives were used: vapors of H_2O, EtOH, Me_2SO_4, $(MeO)_3B$, $(MeO)_3P$, PCl_3, NH_4OH, and HCl. The conditions were chosen in such a way that the content of the introduced substance would be the same in all cases and equal to 5 mmol L^{-1}.

The composition of solid pyrolysis products was determined by elemental analysis using a Vario Micro Cube CHNS/O analyzer and by X-ray diffraction analysis with Dron-1 and ARL X´TRA diffractometers. The structure of carbon nanotubes was studied by transmission electron microscopy (TEM) using EMV-100B and JEOL JEM-100 CX electron microscopes. The composition of gaseous pyrolysis products was determined by mass spectrometry on a MI 1201V instrument (EI, 70 eV). The influence of the gas phase composition during ethylene pyrolysis on the structure of formed carbon nanofibers was studied using TEM.

To determine the size of active catalyst particles, the solid pyrolysis products were studied by X-ray diffraction analysis and electron microscopy. The cluster sizes were calculated from diffraction patterns by the Scherrer equation for the line Ni (200). We failed to reveal any dependence of the catalytic particle size on additives introduced into the reaction zone. The average size of the nature of nickel crystallites calculated from the diffraction patterns was 10—20 nm in all experiments. According to the data of electron microscopy, the average size of catalytic particles located, as a rule, at the edges of carbon fibers was in the range of 10 to 30 nm. Further carbon pyrolysis products were purified from the catalysts and support by ultrasonic treatment in concentrated hydrochloric acid at 70 °C for 1.5 h.

Results and Discussion

The data on the influence of various gaseous additives on the yield of carbon pyrolysis products are presented in Fig. 1. A preliminary control experiment was carried out and carbon nanofibers were obtained by the pyrolysis of a C_2H_4—H_2—Ar (1.5 : 3 : 1, vol.) gas mixture at 700 °C. The mass spectra of the initial gas mixture exhibit peaks with m/z (I_{rel} (%)) 40 $[Ar]^+$ (100) and 20 $[Ar]^{2+}$ (12). In addition, there are peaks with m/z 24, 25, 26, 27, 28, and 29 (maximum peak with m/z 28 $[C_2H_4]^+$), as well as the peak with m/z 2 $[H_2]^+$ (Fig. 2). The spectra of the gaseous

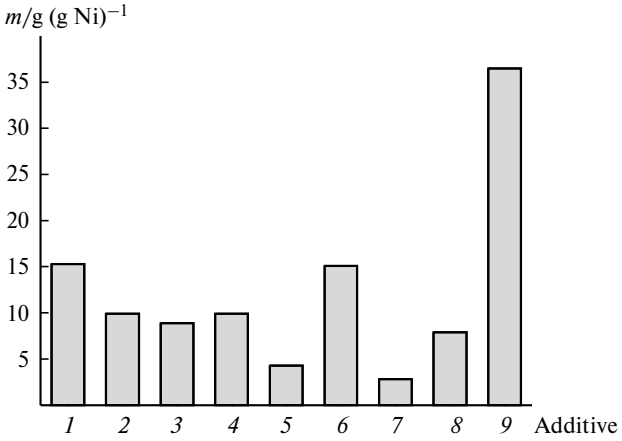

Fig. 1. Influence of additives introduced into the gas phase on the yield of carbon nanofibers at 700 °C: *1*, control experiment; *2*, H_2O; *3*, EtOH; *4*, NH_4OH; *5*, PCl_3; *6*, $(MeO)_3P$; *7*, Me_2SO_4; *8*, $(MeO)_3B$; and *9*, HCl; *m* is the mass of carbon.

pyrolysis products exhibit peaks with m/z 12, 13, 14, 15, 16, 17 $[CH_4]^+$ and m/z 24, 25, 26, 27, 28, 29, 30 $[C_2H_6]^+$ (see Fig. 2). The presence of ethane is indicated by a considerable increase in the intensity of the peak with m/z 29 and the appearance of the peak with m/z 30. Starting from the data obtained, we may assume that several parallel processes can occur during pyrolysis

$$H_2C{=}CH_2 \longrightarrow 2\,C + 2\,H_2, \quad (1)$$

$$H_2C{=}CH_2 \longrightarrow C + CH_4, \quad (2)$$

$$H_2C{=}CH_2 + 2\,H_2 \longrightarrow 2\,CH_4, \quad (3)$$

$$H_2C{=}CH_2 + H_2 \longrightarrow C_2H_6. \quad (4)$$

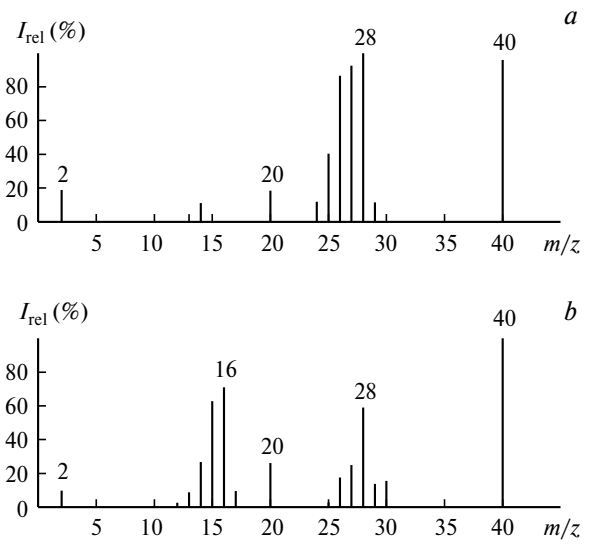

Fig. 2. Mass spectra of the initial gas mixture C_2H_4—H_2—Ar (1.5 : 3 : 1) (*a*) and pyrolysis products at 700 °C (*b*).

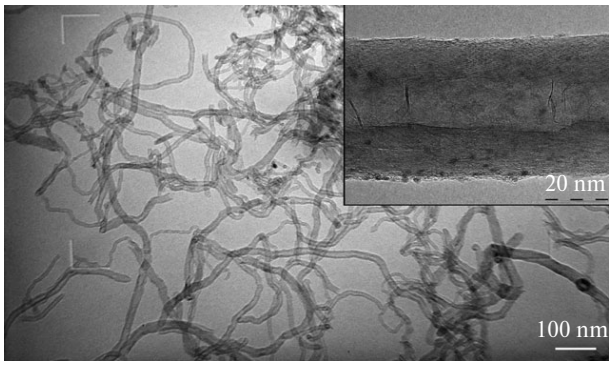

Fig. 3. TEM image of the pyrolysis products of the C_2H_4—H_2—Ar (1.5 : 3 : 1) gas mixture at 700 °C.

Evidently, processes (1) and (2) are target and processes (3) and (4) are side.

Pyrolysis of the gas mixture at 700 °C affords coaxial conic nanofibers of the "Herringbone" type with diameters 10—30 nm (Fig. 3). The channel width in the obtained fibers reaches 15 nm. The yield of carbon products was 15.3 g (g Ni)$^{-1}$.

Upon the addition of water vapor to the initial gas mixture, a peak with m/z 18 $[H_2O]^+$ appears in the mass spectra and the fraction of the peak with m/z 28 increases among the cluster of other peaks of this group in the spectra of the pyrolysis products. Ions $[CO]^+$ and residues of $[C_2H_4]^+$, which did not decompose on the catalyst surface, can contribute to the intensity of this peak (Fig. 4).

The addition of ethanol vapor to the reaction zone results in the additional appearance in the mass spectra of two groups of peaks with maxima at m/z 31 and 45, which are characteristic of the spectrum of ethanol (Fig. 5). The

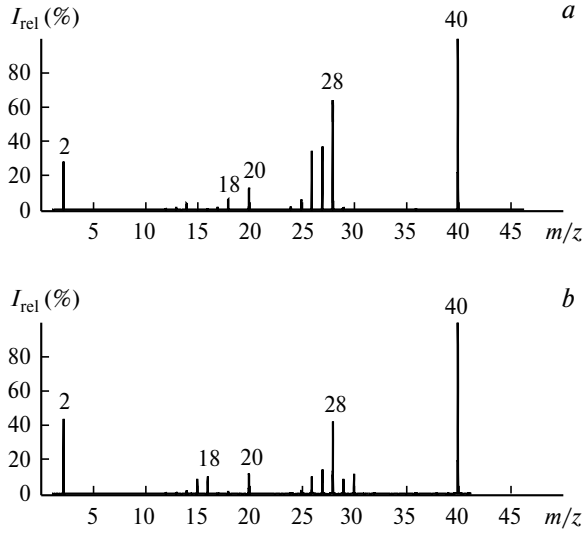

Fig. 4. Mass spectra of the initial gas mixture to which water vapor was added (*a*) and the pyrolysis products (*b*).

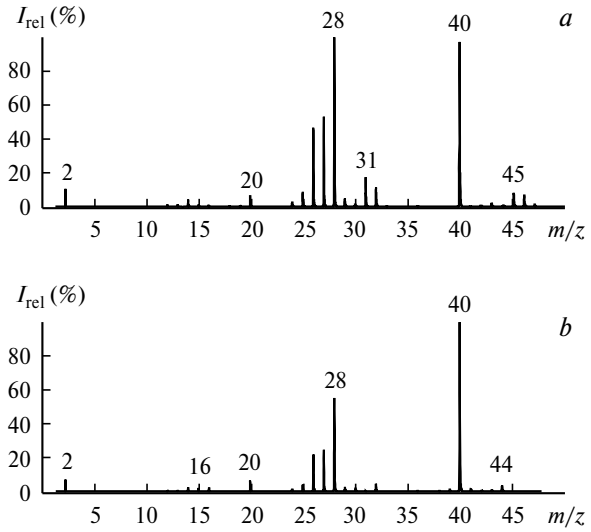

Fig. 5. Mass spectra of the initial gas mixture to which ethanol vapor was added (*a*) and the pyrolysis products (*b*).

mass spectrum of the pyrolysis products contains peaks with m/z 16 $[CH_4]^+$ and 28 and the peak with m/z 44, which can correspond to ions $[CO_2]^+$ and $[C_2H_4O]^+$. Probably, the following reactions related to the presence of ethanol vapor occur during pyrolysis:

$$EtOH \longrightarrow CH_4 + CO + H_2, \quad (5)$$

$$EtOH \longrightarrow C_2H_4O + H_2, \quad (6)$$

$$C_2H_4O \longrightarrow CH_4 + CO, \quad (7)$$

$$2\,CO \longrightarrow C + CO_2. \quad (8)$$

Pyrolysis of ethylene at 700 °C in the presence of water or ethanol vapor affords carbon fibers with a narrower diameter distribution (Fig. 6). Fiber diameters are 10—20 nm on the average and the channel width ranges from 3 to 5 nm. The addition of ethanol vapor affords carbon fibers, whose diameter is somewhat smaller than that of the fibers obtained with the addition of water vapor to the reaction mixture. Many defects are observed in the surface of the fibers. The total yield of the carbon products was 9.9 g (g Ni)$^{-1}$ when using a mixture with the addition of water vapor and 8.9 g (g Ni)$^{-1}$ for a mixture with the addition of ethanol vapor. The presence of many defects on the fiber surface can facilitate the further functionalization of the carbon material.

The addition of ammonia vapor to the initial gas mixture results in the appearance in the mass spectra of the group of peaks with m/z 14, 15, 16, 17, and 18; the peak with the maximum intensity was detected as m/z 17 $[NH_3]^+$ (Fig. 7). In the spectrum of the reaction products, the peak with m/z 28 increases substantially. Along with ethylene residues, ions $[N_2]^+$ and $[CO]^+$ can contribute to

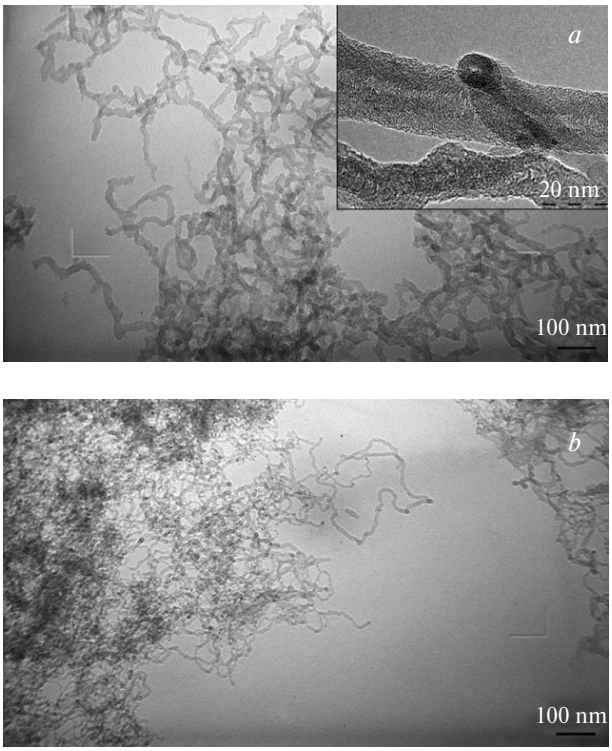

Fig. 6. TEM image of the pyrolysis products of the gas mixture to which water (*a*) and ethanol (*b*) vapors were added.

this peak. The appearance of ions $[N_2]^+$ is due to ammonia decomposition

$$2\,NH_3 \longrightarrow N_2 + 3\,H_2. \qquad (9)$$

The introduction of ammonia vapor to the reaction zone somewhat decreases the total yield of solid pyrolysis products, which was 10.1 g (g Ni)$^{-1}$. Under these conditions, carbon fibers are formed with a diameter of 20—50 nm with channels up to 30 nm in diameter (Fig. 8). Channels have many dams, indicating the "bamboo-like" structure of the fibers. In this case, the carbon fibers grow jumpwise, due to which many dams are formed inside the channels.

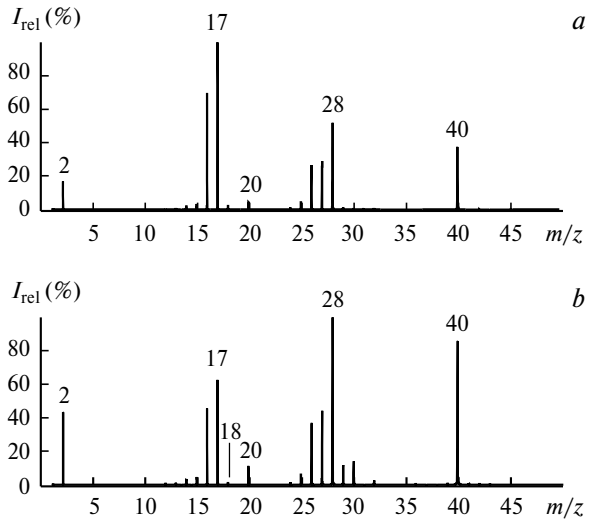

Fig. 7. Mass spectra of the initial gas mixture to which ammonia vapor was added (*a*) and the pyrolysis products (*b*).

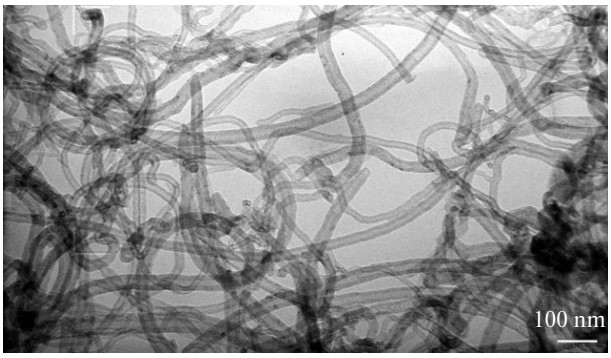

Fig. 8. TEM image of the pyrolysis products of the gas mixture to which ammonia vapor was added.

Two groups of peaks (*m/z* 101, 103, 105 and 136, 138, 140) with maxima at *m/z* 101 and 136 are detected in the mass spectrum upon the addition of phosphorus trichloride to the gas mixture. Two peaks with *m/z* 34 $[PH_3]^+$ and 36 $[HCl]^+$ appear in the mass spectrum of the reaction product (Fig. 9), which is due to the interaction of the starting chloride with hydrogen, resulting in phosphorus hydride and hydrogen chloride.

$$PCl_3 + 3\,H_2 \longrightarrow PH_3 + 3\,HCl \qquad (10)$$

Pyrolysis of the gas mixture in the presence of PCl_3 vapor affords hole fibers with an average diameter of

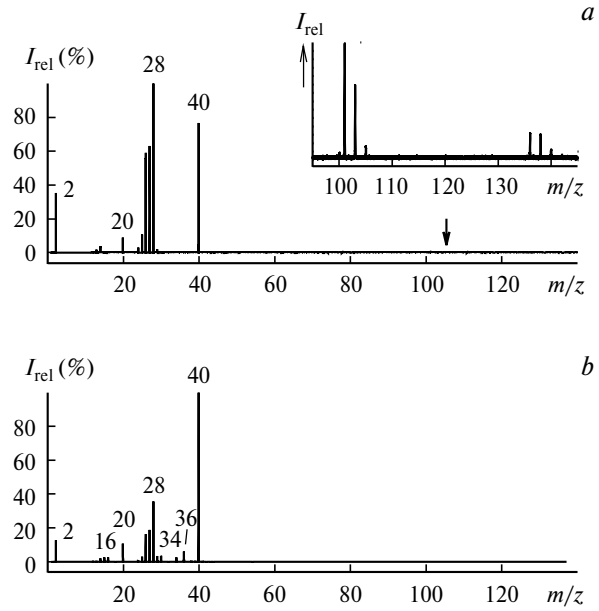

Fig. 9. Mass spectra of the initial gas mixture to which PCl_3 vapor was added (*a*) and the pyrolysis products (*b*).

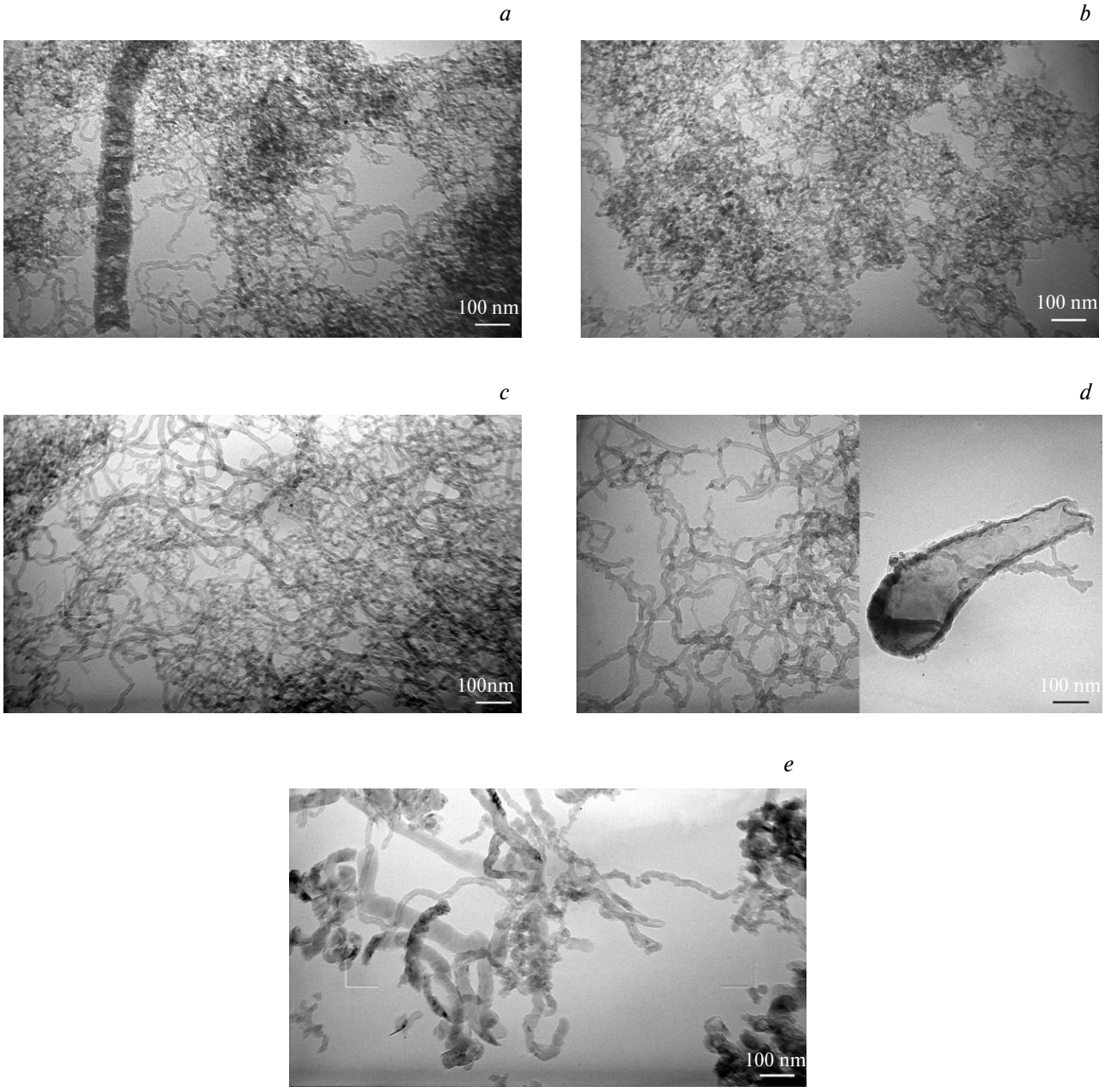

Fig. 10. TEM images of the pyrolysis products of the gas mixture to which PCl_3 (*a*), $(MeO)_3P$ (*b*), Me_2SO_4 (*c*), $(MeO)_3B$ (*d*), and HCl (*e*) vapors were added.

10—15 nm and a channel width of 3—5 nm (Fig. 10, *a*). In particular cases, planar parallel fibers with the diameter up to 150 nm appear along with the above fibers. A similar pattern is observed upon the addition of vapor of methyl phosphonate $(MeO)_3P$ to the initial mixture. Pyrolysis with this additive produces fibers with an average diameter of 10—15 nm (see Fig. 10, *b*). The total yield of the carbon products for the mixture with addition of $(MeO)_3P$ vapor was 15.1 g (g Ni)$^{-1}$.

The lowest yield of the carbon pyrolysis products (2.8 g (g Ni)$^{-1}$) was obtained upon the addition of dimethyl sulfate Me_2SO_4 to the initial gas mixture. This produces hole fibers with diameters of 5—20 nm and a channel width of 2—7 nm (see Fig. 10, *c*). Evidently, sulfur poisons the catalysts, thus favoring the overall decrease in the yield of the target product. It is most likely that the fibers grow predominantly on small particles. Diffusion on them occurs more rapidly, which provides the narrow diameter distribution of the fibers.

The introduction of vapor of methyl orthoborate $(MeO)_3B$ into the reaction zone favors the formation of fibers with diameters of 15—30 nm (see Fig. 10, *d*). Inter-

nal channels of these fibers are broader than usual ones and can reach 15 nm at a fiber thickness of 20 nm. On the average, the channel width is 10 nm. In several cases, large structures with the diameter to 250 nm with the cavity inside reaching 150 nm are formed.

The highest yield with respect to carbon was achieved by the addition of HCl vapor (36.5 g (g Ni)$^{-1}$). In this case, carbon fibers with a larger diameter range varying from 15 to 70 nm were formed (see Fig. 10, *e*). The influence of chlorine atoms on the yield of the carbon products can be explained by the promoting effect.[20] Carbon fibers grow on both large and small catalyst particles, which explains, most likely, a pronounced difference in diameters of the fibers formed. The introduction of PCl_3 vapor to the reaction zone induces no increase in the target product yield. Perhaps, this is related to the fact that the presence of phosphorus trichloride favors coke formation on the working catalyst surface and the growth occurs predominantly on particles 10—15 nm in size, where the rates of diffusion and formation of fibers are considerably higher than on larger particles. This assumption is confirmed by the data of electron microscopy (see Fig. 10, *a*).

According to the elemental analysis data, the hydrogen content in the carbon pyrolysis products is maximum for the fibers obtained with the addition of water or ethanol vapors (1.5%), whereas it is <1% in other cases.

Thus, even a small amount of various additives introduced into the reaction zone of catalytic pyrolysis of ethylene exerts a substantial effect on the yield, structure, and properties of the carbon nanofibers formed. The addition of hydrogen chloride favors an increase in the yield of carbon products, while the introduction of sulfur compounds decreases the yield. The introduction of sulfur- and phosphorus-containing additives facilitates the growth of thinner fibers. "Bamboo-like" fibers are formed in the presence of ammonia, and the addition of water or ethanol results in the appearance of defects on the surface of carbon fibers.

This work was financially supported by the Russian Foundation for Basic Research (Project No. 08-03-01117).

References

1. B. H. Hong, J. Y. Lee, T. Beetz, Y. Zhu, P. Kim, K. S. Kim, *J. Am. Chem. Soc.*, 2005, **127**, 15336.
2. E. G. Rakov, *Nanotrubki i fullereny* [*Nanotubes and Fullerenes*], Logos, Moscow, 2006, 376 pp. (in Russian).
3. T. Ikuno, S. Honda, K. Kamada, K. Oura, M. Katayama, *J. Appl. Phys.,* 2005, **97**, 104329.
4. M. Jung, K. Y. Eun, Y.-J. Baik, K.-R. Lee, J.-K. Shin, S.-T. Kim, *Thin Solid Films*, 2001, **398**—**399**, 150.
5. L. Zhu, Y. Sun, D. W. Hess, C.-P. Wong, *Nano Lett.*, 2006, **6**, 243.
6. P. B. Amama, C. L. Pint, L. McJilton, S. M. Kim, E. A. Stach, P. T. Murray, R. H. Hauge, B. Maruyama, *Nano Lett.,* 2009, **9**, 44.
7. C. Park, R. T. K. Baker, *J. Catal.*, 2000, **190**, 104.
8. E. G. Rakov, *Usp. Khim.*, 2007, **76**, 3 [*Russ. Chem. Rev.* (*Engl. Transl.*), 2007, **76**, 1].
9. Z. Zhou, L. Ci, X. Chen, D. Tang, X. Yan, D. Liu, Y. Liang, H. Yuan, W. Zhou, G. Wang, S. Xie, *Carbon*, 2003, **41**, 337.
10. E. Flahaut, C. Laurent, A. Peigney, *Carbon*, 2005, **43**, 375.
11. F. Benissad-Aissani, H. Aıt-Amar, M.-C. Schouler, P. Gadelle, *Carbon*, 2004, **42**, 2163.
12. S. Y. Brichka, G. P. Prikhod´ko, Y. I. Sementsov, A. V. Brichka, G. I. Dovbeshko, O. P. Paschuk, *Carbon*, 2004, **42**, 2581.
13. Ch. Tang, Y. Bando, D. Golberg, F. Xu, *Carbon*, 2004, **42**, 2625.
14. S. Y. Bae, H. W. Seo, J. Park, Y. S. Choi, J. C. Park, S. Y. Lee, *Chem. Phys. Lett.,* 2003, **374**, 534.
15. T. Luo, J. Liu, L. Chen, S. Zeng, Y. Qian, *Carbon*, 2005, **43**, 755.
16. F. Peng, L. Zhang, H. Wang, P. Lv, H. Yu, *Carbon*, 2005, **43**, 2405.
17. A. A. Volodin, P. V. Fursikov, Yu. A. Kasumov, I. I. Khodos, B. P. Tarasov, *Izv. Akad. Nauk*, *Ser. Khim.*, 2005, 2210 [*Russ. Chem. Bull., Int. Ed.,* 2005, **54**, 2281].
18. A. A. Volodin, *Al´ternativnaya energetika i ekologiya* [*Alternative Power Energy and Ecology*], 2008, **2**, 53 (in Russian).
19. A. A. Volodin, B. P. Tarasov, in *Nanochastitsy v kondensirovannykh sredakh* [*Nanoparticles in Condensed Media*], Ed. P. A. Vityaz´, Izd. Tsentr BGU, Minsk, 2008, 13 (in Russian).
20. H. Qiu, Z. Shi, L. Guan, L. You, M. Gao, S. Zhang, J. Qiu, Z. Gu, *Carbon*, 2006, **44**, 516.

Received August 12, 2010;
in revised form February 2, 2011